Eurographics Conference on Visualization (EuroVis) (2013)
M. Hlawitschka and T. Weinkauf (Editors)

Total Euler Characteristic as a Noise Measure to aid Transfer Function Design

Rafael Wiemker

Philips Research Lab Hamburg

Abstract

For image-based, semi- or fully automated design of transfer functions for direct volume rendering, it is beneficial to have an estimation of the noise level in the rendered image. A topology-motivated noise measure is suggested based on the Euler Characteristic, i.e., on the number of islands and holes in the rendering. The effectiveness of this concept lies in the observation that the Euler Characteristic of the real objects of interest in a rendered scene is usually very low, typically orders of magnitude lower than the Euler Characteristic caused by noise. Interestingly, the Euler Characteristic, which is defined for binary images, can be computed simultaneously for all possible super level sets of an integer-valued gray-scale image in a single raster scan. An efficient algorithm for 2D and 3D is presented with computation cost as low as total variation. The Total Euler Characteristic of the super level sets is proposed as a noise level estimation, i.e., the L1-norm of the evolution curve of the Euler Characteristics for all possible isovalues. The superiority of the Total Euler Characteristic to other common noise estimation methods such as total variation and total second derivatives is demonstrated on renderings of the Marschner-Lobb phantom.

Categories and Subject Descriptors (according to ACM CCS): I.3.3 [Computer Graphics]: Picture/Image Generation—Viewing algorithms

1. Introduction and Motivation

The ability to cope with noise is one of the strengths of direct volume rendering (DVR). Simply by widening the ramp of the opacity transfer function (TF), isosurfaces can often be rendered successfully even in quite noisy image data volumes [HJ05, PB07]. The alternative employment of a prior smoothing of the data volume may require substantial precomputation time, and may also require specific choices of algorithms and parameter settings, and thus entail implicit decisions which are not obvious to the viewer of the apparently smooth rendering. In particular in certain medical imaging use-cases, a direct rendering with implicit noise reduction by soft TFs may be the more trusted solution in view of potential artifacts or erroneous suppressions by too sophisticated preprocessing algorithms or explicite surface segmentations.

In image-driven TF design [PB07], a two-dimensional rendering of a given three-dimensional image volume is generated with a certain TF, then the rendering is analyzed by a human or an algorithm, and the TF is varied iteratively until an optimal result is achieved. A basic primitive of a TF is a simple ramp function which can be parametrized by a level and a window width. For noisy image data, a wide ramp can effectively prevent too early termination of the view rays. On the other hand, the width of the TF ramp should be as narrow as possible in order to preserve the details of the isosurface of interest. To negotiate this trade-off between noise suppression and detail preservation, it is useful to have an automatic and efficient estimation of the noise level in the rendering resulting from a certain TF. A well founded and widely used choice is the total variation (TV) [ROF92, Sze10] which is usually computed as the L1-norm of the local gradients. However, in an unsupervised TF optimization, this may lead to an over-estimation of the noise and thus to an unnecessary loss of rendering details if the object of interest itself contains a significant amount of gradients on its isosurface, which is then mis-interpreted as noise. Another widely used measure which avoids this problem of true gradients is the total amount of second derivatives (L1-norm of the local Laplacian). Again, however, this measure may lead to noise over-estimation and unnecessary loss of detail if the objects of interest does indeed possess a strongly curved isosurface.

DOI: 10.2312/PE.EuroVisShort.EuroVisShort2013.097-101

The visually most obvious sign of noise in a rendering is the presence of tiny bright or dark speckles. If the rendering is binarized into the sub- and super level set at a certain isovalue, these speckles manifest as connected components and holes of the super level set. In algebraic topology, these are known as the first two Betti numbers. The Euler Characteristic χ measures topological complexity and gives only a combination of these two properties

$$\chi = \#\text{islands} - \#\text{holes}$$

but has the advantage to be computable very effciently on binary images [Gra71, LVG80].

In order to analyze the overall noise level of a grayscale –not binary– rendering, we need to analyze the evolution of the Euler Characteristic through all possible super level sets, i.e., for all possible isovalues of the rendered image. Interestingly, for an integer-valued image all these Euler Characteristics can be computed simultaneously for all isovalues in a single raster scan, with computation costs as low as standard total variation, as shown in section 2. This curve, i.e., the topological evolution of the Euler Characteristic $\chi(T)$ as a function of the isovalue T, can serve as a superior noise measure, because the truely relevant –not noise-related– number of connected components and holes in a rendering is typically very low for many practical applications in medical visualization. E.g. for endo-luminal renderings (bronchoscopies, colonoscopies) there typically is only a single connected components with few holes at furcations. In contrast, the number of noise induced speckles may be higher by several orders of magnitude. Thus, the noise estimation by virtue of the Euler Characteristics essentially approximates zero once a good TF has been found, while a significant amount of gradients and curvatures may still remain in the rendering. The latter might be excessively smoothed out by standard noise measures such as total variation, which have a significant non-vanishing offset accounting for the true image content of interest.

As the Euler Characteristic $\chi(T)$ can be positive as well as negative depending on the isovalue T, it is advantageous to use as a scalar noise level estimation the *Total* Euler Characteristic *TEC* , *i.e.*, the L1-norm of the Euler Characteristics of the super level sets for all possible isovalues T:

$$TEC = \sum_T |\chi(T)|$$

The remainder of this paper is organized as follows: The efficient computation of the Euler Characteristic for all super level sets is detailed in section 2, and an example is given to illustrate its behavior. In section 3 experimental results for noise simulations with the Marschner-Lobb phantom are given to demonstrate the effectiveness of the Total Euler Characteristic, and to compare it to total variation, followed by conclusions in section 4.

1.1. Related Work

Topological aspects have been considered previously for TF design in direct volume rendering [WDC*07], however with respect to the contour tree rather than to noise. The Euler Characteristic is an important and well understood topological descriptor, and invariant against translation, rotation, scaling and warping [Loh98, OS06, CGR11]. Formally, it can be described as the sum of the first Betti numbers, for which efficient comptutation methods have been presented [DE93, PCM03]. The Euler Characteristic is one of the Minkowski functionals and has been used successfully in medical imaging for change detection in dynamic sequences [HWK*05], pulmonary texture analysis [HNL*10], bone density analysis [RdSB09], etc. The noise measure described in this paper is conceptually unrelated but algorithmically very similar to the efficient histogram-based computation of the total gradient for all possible level sets presented in [PWH01, WZ01].

2. Efficient Euler Characteristic Computation For All Isovalues Simultaneously

In 2D, the Euler Characteristic can be computed conveniently via the Euler-Poincaré formula [OS06]

$$\chi = \#\text{vertices} - \#\text{edges} + \#\text{faces}$$

A crucial property of the Euler Characteristic is its additivity, so the global Euler Characteristic for a whole image can be summed up from purely local Euler Characteristics, *i.e.*, by a sliding window which checks the vertices, edges, and faces in a 2×2 neighborhood (Fig. 1). In order to achieve this simultaneously for all isovalues T we employ a histogram technique with a histogram variable H[T] with a bin width of one for each possible intensity value I. For explanation, let us consider the isovalue T to start with the highest possible intensity value $T = I_{\max}$. While we lower this isovalue, a vertex at a certain image position (x,y) will become part of the super level set when the isovalue reaches the intensity $I(x,y)$ at this pixel. So the histogram is *in*cremented at this bin I. An edge becomes part of the super level set when the isovalue becomes lower than the pixel and its neighbor, *i.e.*, once the isovalue is lower than the minimum of the two neighboring values. According to the Euler-Poincaré formula, this bin will be *de*cremented. Furthermore, the bin of the minimum intensity of four neighboring pixels forming a face will be *in*cremented. Finally, after the raster scan is concluded, the such filled histogram H is accumulated starting from the highest bin, so that each bin contains the cumulative counts for all vertices, edges and faces which have become part of the super level set so far until the current isovalue has been reached (see pseudo-code in Fig. 1). The algorithm is exact and tractable for integer-valued data such as 8- and 16-bit images. It is conveniently extensible to 3D by considering the next Betti number, which is achieved by *de*crementing the histogram for 8-voxel-cubes in a $2\times2\times2$ neighborhood.

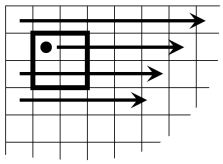

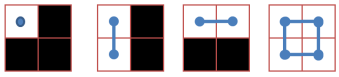


```
// raster scan:
foreach voxel [x,y] in image I:
    H[ I[x,y] ]++; // vertex; increment Euler histogram H
    H[ MIN(I[x,y], I[x+1,y]) ]--; // edge 1
    H[ MIN(I[x,y], I[x,y+1]) ]--; // edge 2
    H[ MIN(I[x,y], I[x,y+1], I[x+1,y], I[x+1,y+1]) ]++; // face

    // optional - extension to 3D:
    H[ MIN(I[x,y,z], I[x,y,z+1]) ]--; // edge 3
    H[ MIN(I[x,y,z], I[x,y+1,z  ], I[x+1,y,z  ], I[x+1,y+1,z  ],
           I[x,y,z], I[x,y+1,z+1], I[x+1,y,z+1], I[x+1,y+1,z+1]
           ) ]--; // cube (additional Betti number for 3D)

// accumulation downwards from highest isovalue:
for (int i = Imax - 2; i >= 0; i--) H[i] += H[i + 1];
```

Figure 1: *Computation of the Euler Characteristic by a raster scan with a sliding 2×2 window, with pseudo-code for efficient computation for all level sets simultaneously, using an Euler-weighted histogram H with bins for all possible isovalues I = [0..I_{max}]. (Extension to 3D with a sliding 2×2×2 window.)*

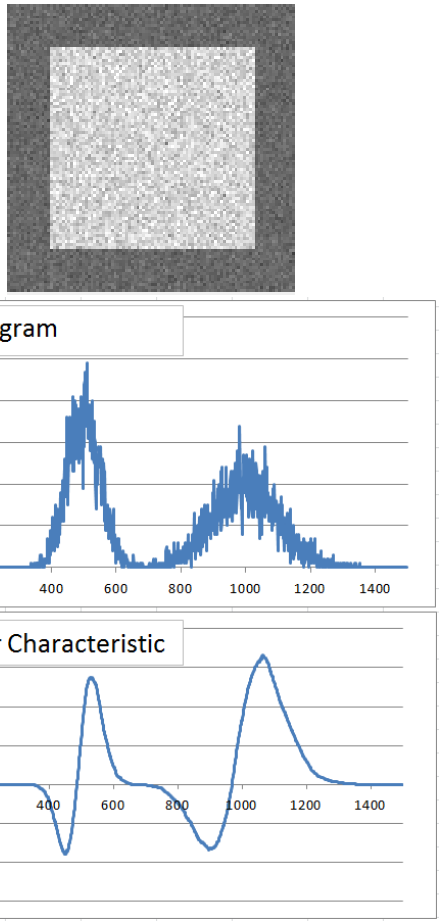

Figure 2: *Example image (integer values 0..1500) with dark and bright area of equal size with multiplicative Gaussian noise, with standard histogram and the topological evolution of the Euler Characteristic $\chi(T)$ as a function of isovalue T.*

In that way it can be applied to the 3D data volume instead of the 2D render image. For completeness it should be mentioned that the Euler Characteristics of the *sub* level sets can be computed analogously by replacing MIN by MAX and inverting the final accumulation order.

2.1. Computation Cost

Apart from the histogram accumulation which is not dependent on the number of pixels in the image and thus negligible, four intensity points have to be sampled for each image pixel (eight for 3D). In comparison, total variation (using a one-sided neighbor scheme in x and y) needs three sample values, and total second derivatives needs five samples (left and right neighbors in x and y).

2.2. Example

Fig. 2 shows a simple example image with multiplicative Gaussian noise. The dark and bright image area are of equal size, but the standard histogram has different peak heights since the noise-distribution is wider for the brighter center area. For each histogram peak, the Euler Characteristic $\chi(T)$ first becomes negative as holes appear for isovalues below the center of the distribution, then positive as islands remain at higher isovalues, with a zero-crossing at the center of the distribution. Note that the curve of the Euler Characteristic is much smoother than the standard histogram.

3. Experimental Results

The Marschner-Lobb phantom [ML94] is a widely used phantom to evaluate rendering techniques [HJ05,PB07]. The phantom was thresholded at 0.5 and Gaussian noise was added of various standard deviations σ (Fig. 3), followed by conversion to integer values by scaling with 1000. For comparison of the response of various noise estimation methods, the depth image of the direct volume rendering in z-direction was used, *i.e.*, the position where the view ray reaches 100% opacity. The depth image –although not shown to the user– is a better measure of isosurface integrity than the final ren-

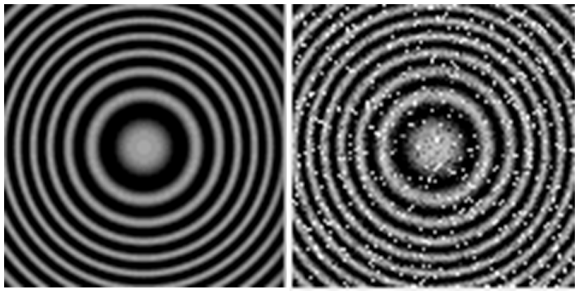

Figure 3: *DVR depth image of the Marschner-Lobb-phantom (left), with Gaussian noise of σ = 40% of the data contrast (right).*

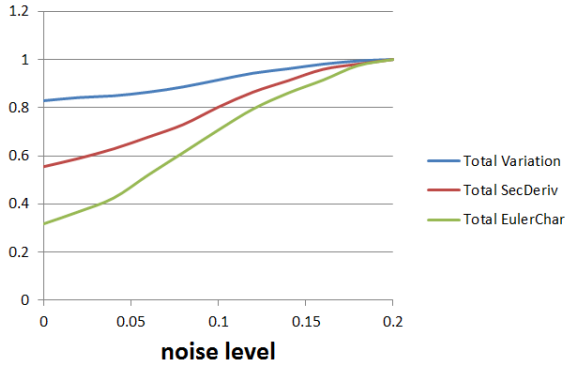

Figure 4: *Response of noise estimation methods to Marschner-Lobb-phantom with different levels of Gaussian noise (abscissa: relative Gaussian σ, ordinate: max response normalized to 1).*

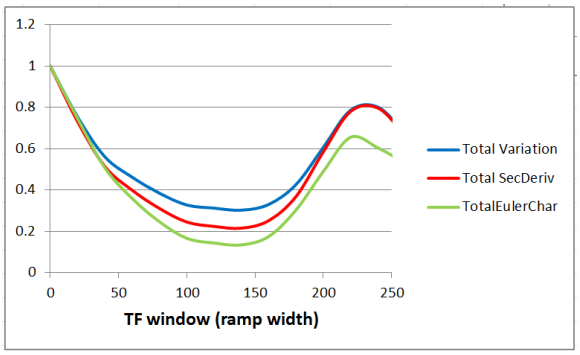

Figure 5: *Noise response to variation of the TF ramp width (Marschner-Lobb-phantom with Gaussian noise σ = 20%, max response normalized to 1).*

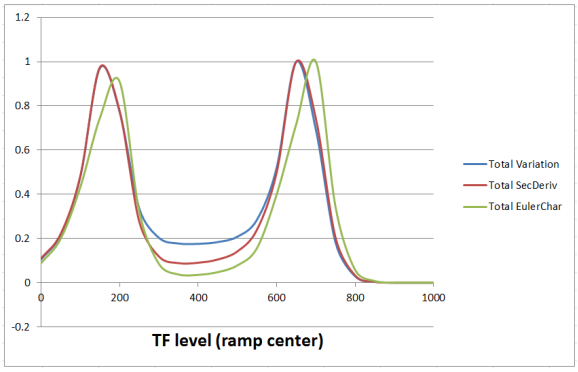

Figure 6: *Noise response to variation of the TF ramp center (Marschner-Lobb-phantom with Gaussian noise σ = 20%).*

dering with shaded and specular lighting. Total variation (TV) was measured as $\sum |I_x| + |I_y|$, and total second derivatives (TSD) as $\sum |I_{xx}| + |I_{yy}|$. Fig. 4 shows that even the TEC does not respond ideally, *i.e.*, with zero to complete absence of noise (because numercial inaccuracies at the thin crests of the ML-phantom produce some speckles). However, the TEC response is significantly lower and thus more reflective of the true noise level than TV and TSD. In another experiment, window (Fig. 5) and level (Fig. 6) of a simple ramp TF were varied, and the resulting rendering evaluated by the three noise estimation methods. The noise minima – desirable for a good TF– are more pronounced for TEC than for TV or TSD.

4. Conclusions and Future Work

An efficiently computable topology based noise measure was presented which is beneficial for automated evaluation of direct volume renderings, and for controlling the parameters of TFs or other smoothing operations. Total Euler Characteristic (TEC), i.e., the L1-norm of the evolution curve of the Euler Characteristic over all super level sets, appears to be a more suitable noise measure than *e.g.* total variation for scenes which contain many true gradients and curvatures, as it better approximates zero for vanishing noise. Furthermore, its topological motivation may be more reflective of human perception of noise in images.

TEC can be computed for 2D in the rendered image for image-centric TF design, or for 3D in the data volume for data-centric TF design. The data-centric approach does not have the view angle dependency which is inherent to image-centric TF design. The practical benefits of TEC for either approach need to be investigated further. The evolution curve of the Euler Characteristics may also be another helpful addition to the Contour Spectrum [BPS97, PWH01].

Extension of the algorithm from integer to floating point data appears straightforward, but the approximation error needs to be analyzed with respect to histogram bin width.

References

[BPS97] BAJAJ C. L., PASCUCCI V., SCHIKORE D. R.: The Contour Spectrum. In *Proc. Eigth conference on Visualization* (1997), VIS '97, IEEE Computer Society Press, pp. 167–172. 4

[CGR11] CURRY J., GHRIST R., ROBINSON M.: Euler calculus with applications to signals and sensing. *AMS Proceedings* (2011). 2

[DE93] DELFINADO C. J. A., EDELSBRUNNER H.: An incremental algorithm for Betti numbers of simplicial complexes. In *Proc. Ninth annual symposium on Computational geometry* (New York, NY, USA, 1993), SCG '93, ACM, pp. 232–239. 2

[Gra71] GRAY S. B.: Local properties of binary images in two dimensions. *IEEE Trans. Comput. 20*, 5 (1971), 551–561. 2

[HJ05] HANSEN C. D., JOHNSON C. R.: *The Visualization Handbook*. Academic Press, 2005. 1, 3

[HNL*10] HUBER M. B., NAGARAJAN M., LEINSINGER G., RAY L. A., WISMÜLLER A.: Classification of interstitial lung disease patterns with topological texture features. In *Proc. SPIE Medical Imaging* (2010), vol. 7624. 2

[HWK*05] HENSEL M., WIESNER G., KUHRMANN B., PRALOW T., GRIGAT R.-R.: Motion detection for adaptive spatio-temporal filtering of medical X-ray image sequences. In *Bildverarbeitung für die Medizin* (2005), pp. 68–72. 2

[Loh98] LOHMANN G.: *Volumetric image analysis*. Wiley, 1998. 2

[LVG80] LOBREGT S., VERBEEK P., GROEN F.: Three-dimensional skeletonization: Principle and algorithm. *IEEE Trans. Pattern Analysis and Machine Intelligence 2*, 1 (1980), 75–77. 2

[ML94] MARSCHNER S. R., LOBB R.: An evaluation of reconstruction filters for volume rendering. In *IEEE Visualization* (1994), pp. 100–107. 3

[OS06] OHSER J., SCHLADITZ K.: *Image Processing and Analysis*. Clarendon Press, 2006. 2

[PB07] PREIM B., BARTZ D.: *Visualization in Medicine. Theory, Algorithms, and Applications*. Morgan Kaufmann, 2007. 1, 3

[PCM03] PASCUCCI V., COLE-MCLAUGHLIN K.: Parallel computation of the topology of level sets. *Algorithmica 38*, 1 (2003), 249–268. 2

[PWH01] PEKAR V., WIEMKER R., HEMPEL D.: Fast detection of meaningful isosurfaces for volume data visualization. In *IEEE Visualization* (2001). 2, 4

[RdSB09] ROQUE W. L., DE SOUZA A. C. A., BARBIERI D. X.: The Euler-Poincaré characteristic applied to identify low bone density from vertebral tomographic images. *Rev Bras Reumatol 49*, 2 (2009), 140–152. 2

[ROF92] RUDIN L., OSHER S., FATEMI E.: Nonlinear total variation based noise removal algorithms. *Physica D 60* (1992), 259–268. 1

[Sze10] SZELISKI R.: *Computer Vision: Algorithms and Applications*. Springer New York, 2010. 1

[WDC*07] WEBER G. H., DILLARD S. E., CARR H., PASCUCCI V., HAMANN B.: Topology-controlled volume rendering. *IEEE Trans. Visualization and Computer Graphics 13*, 2 (2007), 330–341. 2

[WZ01] WIEMKER R., ZWARTKRUIS A.: Optimal thresholding for 3D segmentation of pulmonary nodules in high resolution CT. In *Proc. Computer Assisted Radiology and Surgery (CARS)* (2001), pp. 653–658. 2